Solid State Ionics 266 (2014) 19–24

Contents lists available at ScienceDirect

Solid State Ionics

journal homepage: www.elsevier.com/locate/ssi

Conductivity and oxygen reduction activity changes in lanthanum strontium manganite upon low-level chromium substitution

George Tsekouras *, Artur Braun

Laboratory for High Performance Ceramics, Swiss Federal Laboratories for Materials Science and Technology, Überlandstrasse 129, Dübendorf 8600, Switzerland

A R T I C L E I N F O

Article history:
Received 20 June 2014
Received in revised form 12 August 2014
Accepted 12 August 2014
Available online 1 September 2014

Keywords:
Solid oxide fuel cell
Lanthanum strontium manganite
Chromium poisoning
Electronic conductivity
Electrochemical impedance spectroscopy

A B S T R A C T

On the timescale of solid oxide fuel cell (SOFC) system lifetime requirements, the thermodynamically predicted low-level substitution of chromium on the B-site of (La,Sr)MnO_3 could be a source of cathode degradation underlying more overt and well-known chromium poisoning mechanisms. To study this phenomenon in isolation, electronic conductivity (σ) and electrochemical oxygen reduction activity of the $(La_{0.8}Sr_{0.2})_{0.98}Cr_xMn_{1-x}O_3$ model series ($x = 0, 0.02, 0.05$ or 0.1) were measured in air between 850 and 650 °C. Depending on the extent of chromium substitution and the measurement temperature, electrochemical impedance spectroscopy (EIS) results could be deconvoluted into a maximum of three contributions reflecting possible limiting processes such as oxide ion transport and dissociative adsorption. Chromium substitution resulted in lowered σ (from 174 S cm^{-1} ($x = 0$) to 89 S cm^{-1} ($x = 0.1$) at 850 °C) and a steady rise in associated activation energy (E_a) (from 0.105 ± 0.001 eV ($x = 0$) to 0.139 ± 0.001 eV ($x = 0.1$)). From EIS analyses, ohmic and polarisation resistances increased, whilst E_a for the overall oxygen reduction reaction also increased from 1.39 ± 0.04 eV ($x = 0$) to $1.48–1.54 \pm 0.04$ eV upon chromium substitution.

1. Introduction

Solid oxide fuel cells (SOFCs) are promising for the distributable and efficient conversion of chemical energy (e.g. from natural gas, biogas, liquefied petroleum gas) to electrical energy, and could thus play an important role in lowering greenhouse gas emissions. However, SOFCs can suffer from a number of stability problems, including chromium poisoning of the widely employed cathode based on the perovskite oxide (La,Sr)MnO_3 by chromium-containing metallic alloy interconnects. Numerous studies (e.g. [1–20]) have considered the severity of chromium poisoning of (La,Sr)MnO_3-based cathodes depending on whether the SOFC is operated under load or is held at open-circuit, whether the air supplied to the cathode is dry or humidified, and depending on the interconnect metallic alloy used (Inconel 600, $Cr5Fe1Y_2O_3$, Crofer22APU, RA446, 17–4 stainless steel, AISI 441, SUS430, ITM or ZMG232).

Chromium poisoning of (La,Sr)MnO_3-based SOFC cathodes includes the initial formation of $Cr_2O_{3(s)}$ on the interconnect surface, volatilisation of $Cr_2O_{3(s)}$ to $CrO_{3(g)}$ and $CrO_2(OH)_{2(g)}$, reaction of chromium species with (La,Sr)MnO_3, and deposition of volatile chromium species as $Cr_2O_{3(s)}$ at triple-phase-boundary (TPB) active sites. Regarding the reaction of chromium species with (La,Sr)MnO_3, the formation of the spinel $(Cr,Mn)_3O_4$ is generally observed in chromium poisoning experiments. By extension, the formation of $(Cr,Mn)_3O_4$ is accompanied by the formation of (La,Sr)(Cr,Mn)O_3 according to the equations below [2], which describe the reaction of (La,Sr)MnO_3 with solid (1) or gaseous (2) chromium species:

$$1.5\ Cr_2O_{3(s)} + 3(La,Sr)MnO_3 \rightarrow 3(La,Sr)\left(Cr_{1-y}Mn_y\right)O_3 + \left(Cr_yMn_{1-y}\right)_3O_4 + 0.25\ O_2 \quad (1)$$

$$3\ CrO_{3(g)} + 3(La,Sr)MnO_3 \rightarrow 3(La,Sr)(Cr_{1-y}Mn_y)O_3 + (Cr_yMn_{1-y})_3O_4 + 2.5\ O_2 \quad (2)$$

Another possible route to (La,Sr)(Cr,Mn)O_3 was raised in a study considering the thermodynamics of chromium poisoning in SOFC cathodes [21], where it was predicted that at typical SOFC operating temperatures chromium can be dissolved into (La,Sr)MnO_3 without forming other phases and with the corresponding advent of A-site deficiency according to:

$$(La_{0.8}Sr_{0.2})MnO_3 + 0.1\ CrO_{3(g)} \rightarrow 1.1(La_{0.8}Sr_{0.2})_{0.909}(Cr_{0.091}Mn_{0.909})O_3 \quad (3)$$

Although thermodynamically predicted, chromium substitution into the perovskite lattice of (La,Sr)MnO_3 has not been observed during the

---

* Corresponding author. Tel.: +41 58 765 4952.
E-mail address: george.tsekouras@empa.ch (G. Tsekouras).

http://dx.doi.org/10.1016/j.ssi.2014.08.006

course of chromium poisoning experiments, suggesting slow kinetics [21]. Assuming slow kinetics, the non-observation of chromium-substituted (La,Sr)MnO_3 is not surprising considering that exposure times in all but one (Menzler et al. [13], 8000 h exposure time) of the above-cited chromium poisoning studies were $\leq$3000 h and therefore short compared to SOFC system lifetime requirements, which exceed 40,000 h [20,22]. Moreover, it would be nearly impossible to distinguish any chromium-substituted (La,Sr)MnO_3 formed from (La,Sr)MnO_3 using the common technique of X-ray diffractometry (XRD), since these materials are isostructural on account of the fact that the ionic radii [23] of VI-coordinate (high spin) Mn^{3+} (0.645 Å) and Cr^{3+} (0.615 Å) are similar. Considering that SOFC system lifetime requirements are quite long, the thermodynamically predicted and seemingly slow process of chromium-substituted (La,Sr)MnO_3 formation could be a source of performance degradation underlying more overt and well-known chromium poisoning mechanisms.

To study in isolation the possible degradation of SOFC cathode performance due to the reaction of chromium species with (La,Sr)MnO_3, the present study considers the electronic conductivity (σ) and electrochemical oxygen reduction activity of (La,Sr)MnO_3 into which chromium was systematically substituted at low levels ($\leq$0.1) for manganese on the B-site. Regarding electronic properties, these materials differ considerably compared to widely utilised LSCM SOFC electrode materials, such as the $La_{0.75}Sr_{0.25}Cr_{0.5}Mn_{0.5}O_3$ composition reported by Tao and Irvine [24], since the low-level concentrations of chromium on the B-site are well below the percolation threshold (0.33). Electronic conductivity was considered using the results of electrical conductivity measurements, since the ionic conductivity of (La,Sr)MnO_3 is known to be several orders of magnitude lower in comparison [25]. In order to achieve the aims of the present study the $(La_{0.8}Sr_{0.2})_{0.98}Cr_xMn_{1-x}O_3$ model series ($x = 0, 0.02, 0.05$ or 0.1) was investigated in air over the temperature range 850–650 °C. The somewhat modest maximum extent of chromium substitution ($x = 0.1$) was chosen since Eq. (3) [21] suggests that a substitution level approaching 10% is thermodynamically possible.

2. Experimental

The $(La_{0.8}Sr_{0.2})_{0.98}Cr_xMn_{1-x}O_3$ model series was prepared via solid state synthesis using stoichiometric amounts of La_2O_3, $SrCO_3$, Cr_2O_3 and Mn_2O_3. Prior to accurate weighing of precursor powders, La_2O_3 was decarbonised at 900 °C, whilst $SrCO_3$, Cr_2O_3 and Mn_2O_3 were dried at 300 °C. Powders were mixed in a mortar and pestle with acetone and dried before calcination at 1000 °C for 12 h. Calcined powder mixtures were ground in a mortar and pestle followed by uniaxial pressing under 150 MPa load into pellets that were fired at 1300 °C for 12 h. Fired pellets were ground in a mortar and pestle and resultant powders planetary ball-milled in isopropanol using Ø 3 mm zirconia balls at 400 rpm for 1 h. Recovered powders were uniaxially pressed, fired and milled as above. An additional planetary ball-milling step in isopropanol was carried out using Ø 1 mm zirconia balls at 400 rpm for 0.5 h in order to lower particle size and therefore improve sinterability of final powders. Room temperature powder XRD was performed on a PANalytical X'Pert Pro diffractometer operated in reflection mode using Cu-Kα_1 radiation, 2θ range 20–80°, 0.017° step and 1 h scan duration.

Pellets for van der Pauw electrical conductivity measurements were prepared by mixing ~3.3 g $(La_{0.8}Sr_{0.2})_{0.98}Cr_xMn_{1-x}O_3$ powder, 3× drops of KD-6 liquid polymeric surfactant and acetone in a mortar and pestle. Dried mixtures were uniaxially pressed under 150 MPa load into pellets that were fired at 1300 °C for 12 h, yielding pellets with 78–84% relative density. Measurements were performed under constant air flow on cooling from 850 °C to 650 °C using Pt wire connections, a ProboStat™ unit (NorECs AS) inserted into the hot zone of a vertical furnace, and a multimeter (Keithley 2750).

Symmetrical cells for electrochemical oxygen reduction activity measurements were prepared in triplicate and based on a dense 8 mol% yttria-stabilsed zirconia (YSZ) electrolyte with electrodes on either side composed of active composite (La,Sr)(Cr,Mn)O_3/YSZ and current-collecting pure (La,Sr)(Cr,Mn)O_3 layers. Composite (La,Sr)(Cr,Mn)O_3/YSZ active layers were used to make the experiments technologically relevant and to minimise possible microstructural variation brought about by any changes in the sinterability of (La,Sr)MnO_3 upon chromium substitution. The architecture of symmetrical cells was (La,Sr)(Cr,Mn)O_3/((La,Sr)(Cr,Mn)O_3/YSZ)//YSZ//((La,Sr)(Cr,Mn)O_3/YSZ)/(La,Sr)(Cr,Mn)O_3. The extent of chromium substitution in the active and current collecting layers was matched for each value of x in the $(La_{0.8}Sr_{0.2})_{0.98}Cr_xMn_{1-x}O_3$ model series. Dense YSZ pellets with Ø 20 mm and 2 mm thickness were prepared by uniaxially pressing 3.6 g commercial YSZ powder under 35 MPa load followed by firing at 1450 °C for 12 h. For each composite (La,Sr)(Cr,Mn)O_3/YSZ (50:50 by weight) and pure (La,Sr)(Cr,Mn)O_3 screen-printing ink 1.0 g ceramic was dispersed in acetone with 2 wt.% KD-1 dispersant using an ultrasonic probe for 10 min. To this dispersion was added 0.43 g vehicle consisting of 5 wt.% poly(vinyl butyrate) in terpineol, giving a ceramic: vehicle weight ratio of 70:30. The mixture was magnetically stirred at room temperature overnight to evaporate the acetone and yield the final ink. Composite (La,Sr)(Cr,Mn)O_3/YSZ and pure (La,Sr)(Cr,Mn)O_3 inks were each screen-printed through a 325 mesh to 2× layers thickness in Ø 12 mm disc shape on either side of dense YSZ pellets with drying between the application of layers. Symmetrical cells were fired at 1000 °C for 2 h. Cross-sectional scanning electron microscopy

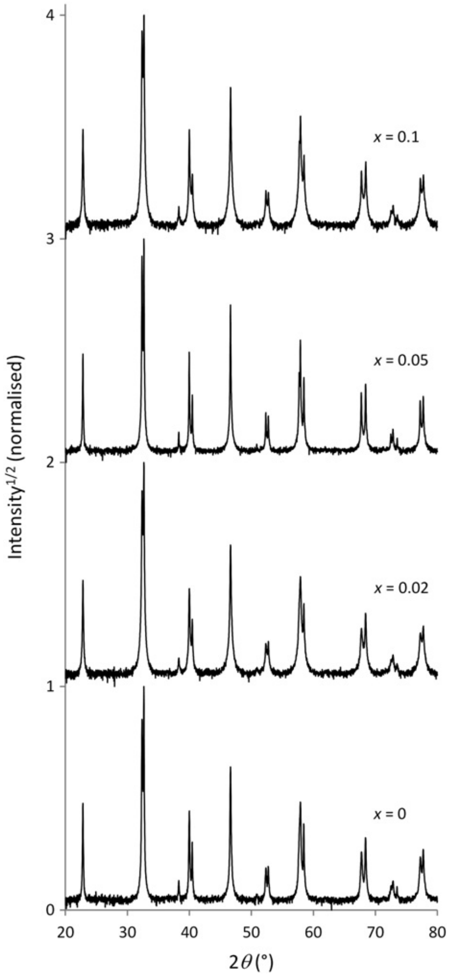

Fig. 1. X-ray diffraction patterns of $(La_{0.8}Sr_{0.2})_{0.98}Cr_xMn_{1-x}O_3$ powders prepared in air via solid state synthesis, with extent of chromium substitution (x) as indicated.